EPJ Web of Conferences **45**, 01035 (2013)
DOI: 10.1051/epjconf/20134501035


# Flow control behind a circular cylinder via a porous cylinder in deep water

B. Gozmen[1, a], E. Fırat[1], H. Akilli[1] and B. Sahin[1]

[1]Department of Mechanical Engineering, Çukurova University, TR 01330, Adana, Turkey

**Abstract.** In this present work, the effects of surrounding outer porous cylinder on vortex structure downstream of a circular inner cylinder are investigated experimentally in deep water flow. The porosity of outer cylinder were selected as $\beta$ = 0.4, 0.5, 0.6, 0.65, 0.7, 0.75, 0.8 and 0.85. Porosity is defined as the ratio of the gap area on the body to the whole body surface area. The ratio of outer cylinder diameter to inner cylinder diameter, $D_o/D_i$ was selected as 2.0, i.e. the inner cylinder diameter is $D_i$ = 30 mm where the outer cylinder diameter is $D_o$ = 60 mm. All experiments were carried out above a platform. The water height between the base of the platform and the free surface was adjusted as 340 mm. Free stream velocity is $U$ = 156 mm/s, which corresponds to the Reynolds number of $Re_i$ = 5,000 based on the inner cylinder diameter. It has been observed that the outer porous cylinders have influence on the attenuation of vortex shedding in the wake region for all porosities. The turbulent intensity of the flow is reduced at least 45% by the presence of outer porous cylinder compared to the bare cylinder case. The porosities $\beta$ = 0.4 and 0.5 are most suitable cases to control the flow downstream of the circular cylinder.

## 1 Introduction

In recent years, the flow around bluff body has been a subject of interest to engineers because of its engineering significance. Researchers concentrate on the control of vortex shedding behavior behind the bluff bodies which cause to flow-induced vibration, acoustic noise, and resonance by increasing the mean lift and drag fluctuations. Most of the studies including vortex shedding are performed on the cylinders having two-dimensional flow structure and ease of arrangements during experimental and computational studies. In order to prevent the problems due to the vortex shedding, there are two main flow control techniques: active and passive control. Active control methods are based on applying some sorts of external energy into the flow field while the passive control techniques control the vortex shedding by modifying the shape of the bluff body or by attaching additional devices in the flow. Splitter plates, small rods, base bleed, roughness elements and helical wires are examples of passive control techniques. There are many numerical and experimental passive control studies for both shallow water and deep water. Lee and Kim [1] investigated the flow characteristics of the wake behind a circular cylinder ($D$ = 40 mm) helically wrapped with three small wires ($d$ = 0.075 $D$; $d$ is the wire diameter) with pitches of 5 $D$ and 10 $D$. They revealed that the surface protrusions elongated the vortex formation region, and decreased the vortex shedding frequency and wake width. Kahraman et al. [2] searched vortex formation of a vertical cylinder in shallow water and the control technique of these vortices. In order to control vortex formation behind a cylinder, they placed a narrow transverse strip of roughness elements having different heights behind the cylinder on the bottom surface channel. They performed a technique of high-image-density particle image velocimetry (PIV) to obtain global, instantaneous representations of the flow patterns. Lim and Lee [3] investigated the flow characteristics of the wakes behind circular cylinders fitted with o-rings. When a circular cylinder fitted with o-rings was compared with the smooth cylinder, the vortex formation region behind the o-ring cylinder was elongated and the width of the wake was decreased. These effects were enhanced with increasing the Reynolds number, decreasing the o-ring diameter and decreasing the pitch, within the experimental conditions tested in their study. Lee et al. [4] investigated experimentally the effects of installing a small control rod upstream of a circular cylinder with a focus on the drag characteristics and the wake structure behind the cylinder. They obtained the form drag coefficient with integrating the surface pressure on the cylinder surface. They found the critical pitch distance $L_c$ at which vortices start to shed from the control cylinder to

[a] bgozmen@cu.edu.tr

obey the relation $L_c/D = 1.5 + 0.083\ d$. Akilli et al. [5] investigated the effect of splitter plate on the suppression of vortex shedding in shallow water by using PIV Technique. Their study denoted that the splitter plate having different thickness presented the same influence on the flow characteristics. The splitter plate had a substantial effect on suppression of the vortex shedding for the gap ratio between 0 and 1.75 *D*. When the splitter plate was located at 2 *D* location, no effect of the splitter plate was observed. Akilli et. al. [6] researched the flow characteristics of the wakes behind the circular cylinder by attaching splitter plates. Their work indicated that the frequency of vortex shedding decreased until the length of $L/D = 0.6$ by lengthening the used splitter plate. Because of the stabilizing effect of the shallow water, the dominant frequency of the shedding vortices was not obtained after the case of $L/D = 0.6$. Until the length of $L/D = 1.2$, the change in the turbulent kinetic energy, Reynolds shear and normal stress patterns were seen negligible. Over this critical length $L/D = 1.2$, the large scale vortex shedding behind the cylinder vanished. Bhattacharrya et al. [7] studied on porosity formation on the body which is another method to control the vortex shedding behind the bluff body. They studied on the flow and concentration field in and around a permeable cylinder has been made through a single domain approach. They found that the drag experienced by the porous cylinder reduces monotonically with the increase of *Re* and decrease of *Da*. The reduction in $C_D$ due to the increase of permeability is more pronounced in the lower range of Reynolds Number. Anderson and Szewezyk [8] experimentally investigated a similar circular cylinder and splitter plate configuration at higher Reynolds numbers. They revealed that the vortex shedding frequency from a circular cylinder with a splitter plate was altered in different ways depending on the length of splitter plate. Yucel et al. [9] studied on interaction of circular cylinder wake with a short located downstream plate. They carried out experiments by Digital Particle Image Velocimetry (DPIV) for Reynolds Numbers of 200, 400 and 750, based on the circular cylinder diameter *D*. This study displayed the interaction of vortices emanating from a circular cylinder with a short downstream plate and their reflection on the frequency and the formation length of the vortices from the cylinder as a function of vertical and horizontal distances between the cylinder and plate. Stappenbelt [10] investigated the proposed utility of splitter-plate wake stabilization as a passive control mechanism for vortex-induced vibration (VIV) mitigation for low aspect ratio cylinders. His experiments of Stationary cylinder show the effectiveness of splitter plates in reducing lift and drag coefficients for a cylinder in uniform flow. On the other hand, rigid attached splitter plates are capable of entirely eliminating vortex shedding in fixed cylinder investigations. Bruneau and Mortazavi [11] performed a new passive control strategy, which consisted of implementing a porous layer between the bluff body and the fluid, in order to change the boundary layer characteristics. The porous medium permeability was directly related to the parameter *K* of the penalization term added to the Navier–Stokes equations. The parametric study showed on the one hand that a wide range of the permeability coefficients (*K*) yielded a significant control of the flow and on the other hand that a sufficient thickness was needed to achieve a good control. Hu and Zhou [12] measured the wake of asymmetric bluff bodies using particle image velocimetry, laser Doppler anemometry (LDA), load cell, hotwire, and flow visualization techniques at *Re* = 2,600-8,500 based on the freestream velocity. They revealed that with increasing corner radius, the flow reversal region is expanded and the vortex formation length is prolonged. Accordingly, the vortex shedding frequency increases and the base pressure rises, resulting in a reduction in the mean drag as well as the fluctuating drag and lift. It is further found that, as the asymmetric cross section of the cylinder causes the wake centerline to shift toward the sharp corner side of the bluff body, the wake remains globally symmetric about the shifted centerline. A numerical study on the laminar vortex shedding and wake flow due to a porous-wrapped solid circular cylinder has been made by Bhattacharyya and Singh [13]. The laminar vortex shedding behind a porous-wrapped solid cylinder was investigated for Reynolds number up to 250. The flow remains symmetric about the central line for this range of Reynolds number and hence the average lift coefficient is found to be zero. Inclusion of a porous wrapper weakens the strength of the separated shear layers and hence delays the vortex shedding. The porous wrapper reduces the pressure drop and skin friction which leads to a reduction in drag compared with a solid cylinder of equal radius.

As instances for deep water studies, Gim et al. [14] studied on flow control by rods of various sizes attached to the rearward stagnation point of a circular cylinder using PIV technique. They performed experiments at Reynolds numbers between *Re* = 5,000 and *Re* = 20,000 based on free stream velocity and the main circular cylinder diameter (*D* = 50 mm). They observed that the wake formation behind a cylinder was influenced by the interaction between the upper and lower sides of the wake, due to the effect of the control rods. Each control rod had distinctive characteristics. However, there was no one optimum control rod for all Reynolds numbers. Galvao et al. [15] tried to control flow using two-dimensional hydrofoils to reduce vortex-induced vibrations (VIV) and drag on a cylinder of circular cross-section. They succeed to completely eliminate vibrations and reduce the drag coefficient to about $C_D = 50$ at sub-critical Reynolds numbers. To control Karman vortex shedding, Schumm et al. [16] performed different experimental control methods in the wake of different two-dimensional bluff bodies, namely an oblong cylinder, circular cylinders and plates of rectangular cross-section. They showed that the coefficients of the Stuart–Landau equation are independent of the experimental technique used to produce the transients. Sahin and Ozturk [17] investigated the nature of the horseshoe vortex system and its interaction with the wake-flow region in the base of circular cylinder mounted on a base plate in deep water. They used the PIV technique to obtain the flow characteristics. Reynolds stress correlations and fluctuations of the velocity components clearly show that the flow structure occurred in the base of the cylinder is

three dimensional. The area of flow field occupied and affected by the horseshoe vortex system around the cylinder varies as a function of Reynolds number.

The present work aims to examine experimentally the effects of surrounding outer porous cylinder on vortex structure downstream of a circular inner cylinder in deep water flow.

## 2 Experimental Set-up and Measurement Techniques

Experiments were performed in a recirculating free surface water channel, having dimensions of 8,000 mm × 1,000 mm × 750 mm, located at Çukurova University, Fluid Mechanics Laboratory of Mechanical Engineering Department, Turkey. The model of water channel is shown in figure 1. Experiments were performed in two steps: Dye visualization experiments and PIV. At the first step, flow visualization experiments were performed using Rhodamine type dye that shines under the continuous laser beam in the desired flow field. Visualization of the experimental results was captured with a high speed SONY 80X handycam type digital video recorder. In the second step, the PIV technique is employed to calculate instantaneous and mean velocity field behind a circular cylinder in order to understand the effect of the porous cylinders on the vortex shedding behavior in deep flow. Particle Image Velocimetry (PIV) is a laser based flow measurement technique which can give quantitative information on the structure of the instantaneous velocity field in a flow plane of interest. By using instantaneous velocity vector field, average velocity field, vorticity contours, Reynolds Stress contours, streamline topology and turbulent statistics could be calculated.

Figure 2 shows the schematic placement of inner cylinder and outer porous cylinder. The porosity of outer cylinder were selected as $\beta$ = 0.4, 0.5, 0.6, 0.65, 0.7, 0.75, 0.8 and 0.85. Porosity is defined as the ratio of the gap area on the body to the whole body surface area. The ratio of outer cylinder diameter to inner cylinder diameter, $D_o/D_i$ was selected as 2.0, i.e. the inner cylinder diameter is $D_i$ = 30 mm where the outer cylinder diameter is $D_o$ = 60 mm. The total depth of the water in the channel was adjusted to a 560 mm height. All experiments were carried out above a platform. The water height between the base of the platform and the free surface was adjusted as 340 mm. Free stream velocity is $U$ = 156 mm/s, which corresponds to the Reynolds number of $Re_i$ = 5,000 based on the inner cylinder diameter.

The measurements were performed and the data were processed using Dantec Dynamics PIV system and Flow Manager Software installed on a computer. The measurement field was illuminated by a thin and an intense laser light sheet by using a pair of double-pulsed Nd:YAG laser units each having a maximum energy output of 120 mJ at 532 nm wavelength. The laser sheet was oriented parallel to the bottom surface of the water channel and the experiments were carried out at the mid-section of cylinder. An 8-bit cross-correlation CCD camera having a resolution of 1,600 × 1,200 pixels, equipped with a Nikon AF Micro 60f/2.8D lens captured the image. In the image processing, 32 × 32 pixels rectangular effective interrogation windows were used. During the interrogation process, an overlap of 50% was employed in order to satisfy Nyguist criterion. A total of 3,844 (62 × 62) velocity vectors were obtained for an instantaneous velocity field at a rate of 15 frames per second (fps). For all experiments, two views one after the other were taken and every field of view was 200 × 200 $mm^2$. The time interval between pulses was 1.5 ms for all experiments and the thickness of the laser sheet illuminating the measurement plane was approximately 2 mm. The water was seeded with the neutrally buoyant spherical particles of 12 μm in diameter. In each experiment, 350 instantaneous images were captured, recorded and stored in order to obtain averaged-velocity vectors and other statistical properties of the flow field. The uncertainty in velocity relative to the depth-averaged velocity is about 2% in these experiments.

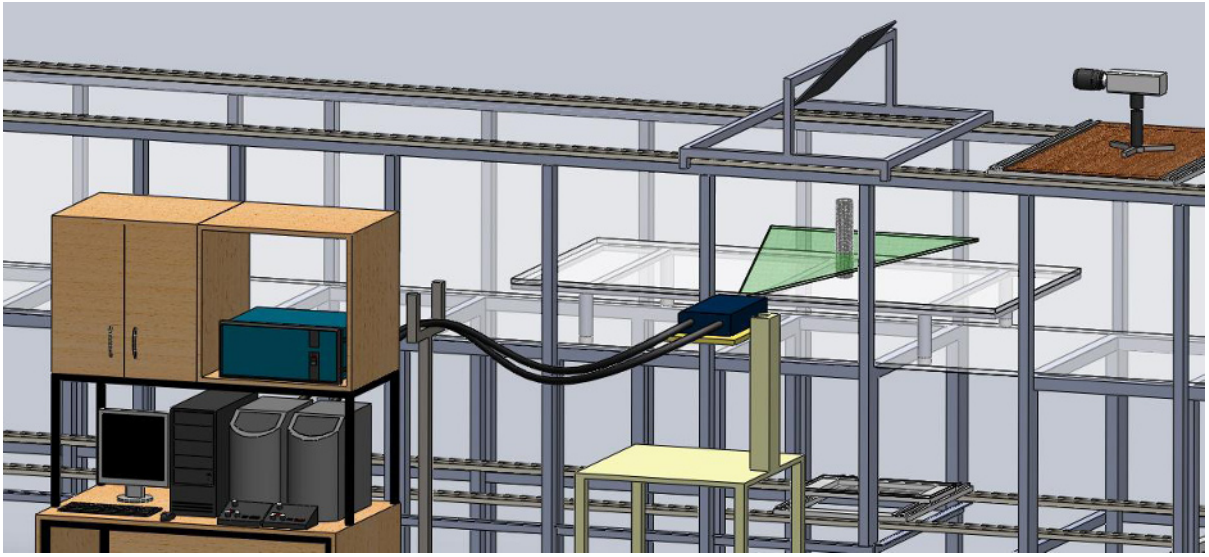

**Fig. 1.** Schematic representation of water channel

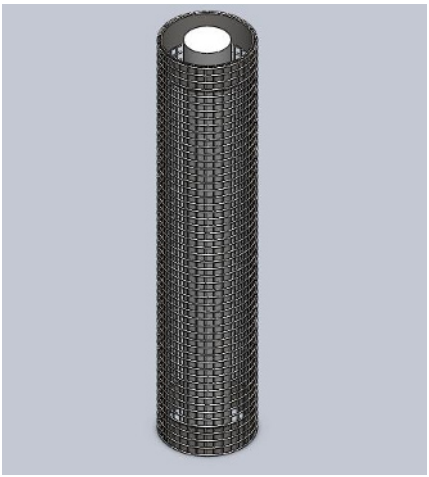

**Fig. 2.** Schematic placement of inner cylinder and outer porous cylinder

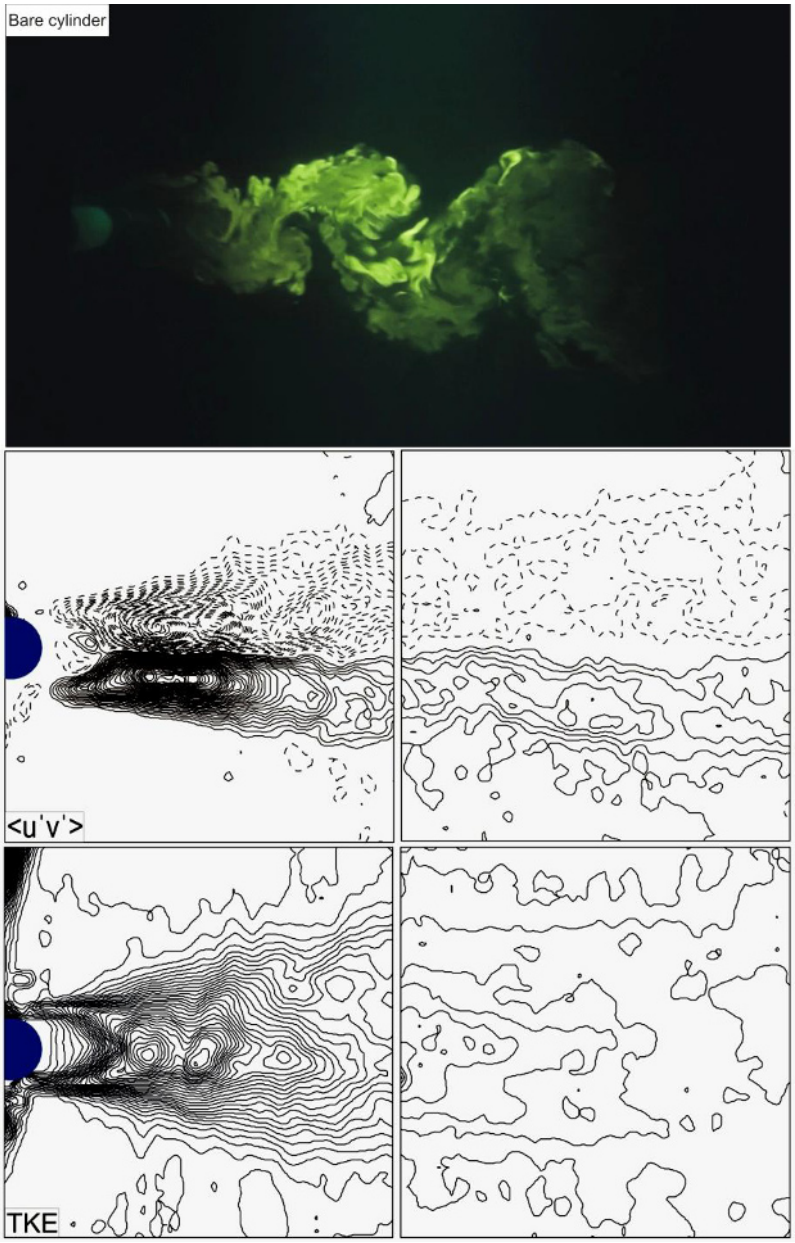


**Fig. 3.** Instantaneous dye image and results obtained from PIV for the bare cylinder

## 3 Results and Discussion

By this study, control of the unsteady flow structure behind a circular cylinder having $D_i$ = 30 mm diameter in deep water was intended. Dye visualization experiments are carried out before PIV experiments to gain quantitative insight about the flow structure behind porous cylinders having various porosities. At first, flow characteristics of bare (inner) cylinder are investigated to compare with the inner cylinder-porous outer cylinder arrangements. To explain the flow structure, the instantaneous dye image, normalized Reynolds stress contours $\langle u' v' \rangle$ and dimensionless turbulent kinetic energy (TKE) contours are shown as seen in figure 3. The dye image shows that well-known Karman Vortex Street occurs downstream of the cylinder. The minimum and incremental values of Reynolds Stress are selected as ± 0.001 and 0.001. The solid and dashed lines present positive and negative Reynolds stress contours, respectively. It is seen that both the negative and positive Reynolds stress contours extend symmetrically along the centerline of the cylinder. The peak value of Reynolds stress is approximately 0.0405 and it occurs in the first view field where the inner cylinder-outer cylinder arrangement is located in. For the turbulent kinetic energy contours, both minimum and incremental values are selected as 0.005. And the maximum dimensionless turbulent kinetic energy value is 0.162 in the first view field.

The qualitative dye images of the flow field for $0.4 \leq \beta \leq 0.85$ are shown in figure 4 to understand the effect of the porosity on the flow structure. It is seen that the vorticity values of $\beta$ = 0.40 and 0.50 prevent the formation of Von-Kármán vortex street downstream of the cylinders. However, the Kelvin-Helmholtz vortices still exist clearly along the shear layer of the outer cylinder. For the porosity range of $0.6 \leq \beta \leq 0.75$, the occurrence of the Von-Kármán vortex street moves away from the cylinders and the flow in the wake region forms like "S" shape. For higher porosities $\beta \geq 0.8$, an unsteady flow structure with smaller frequency compared to the bare cylinder occurs.

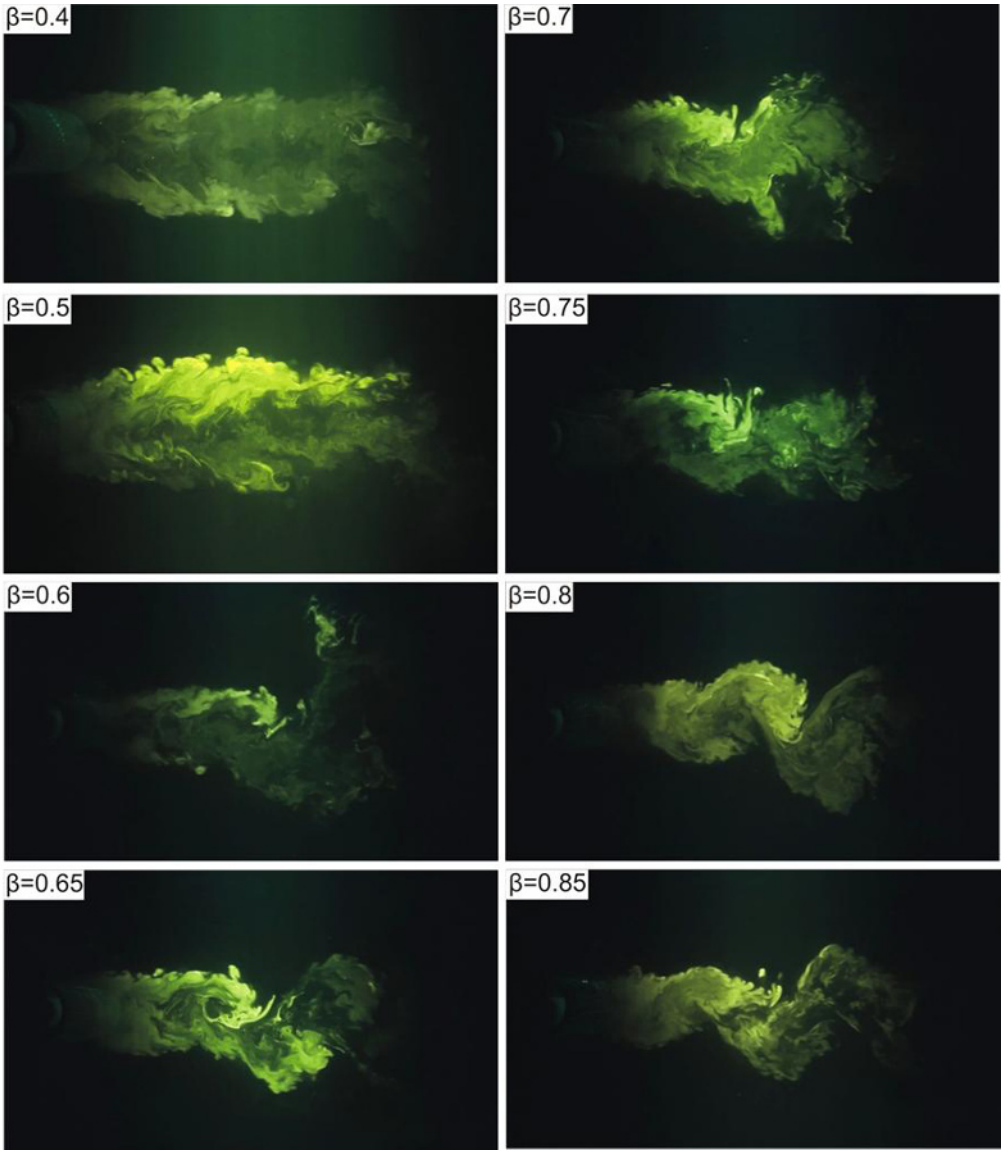


**Fig. 4.** Dye images for all porosities

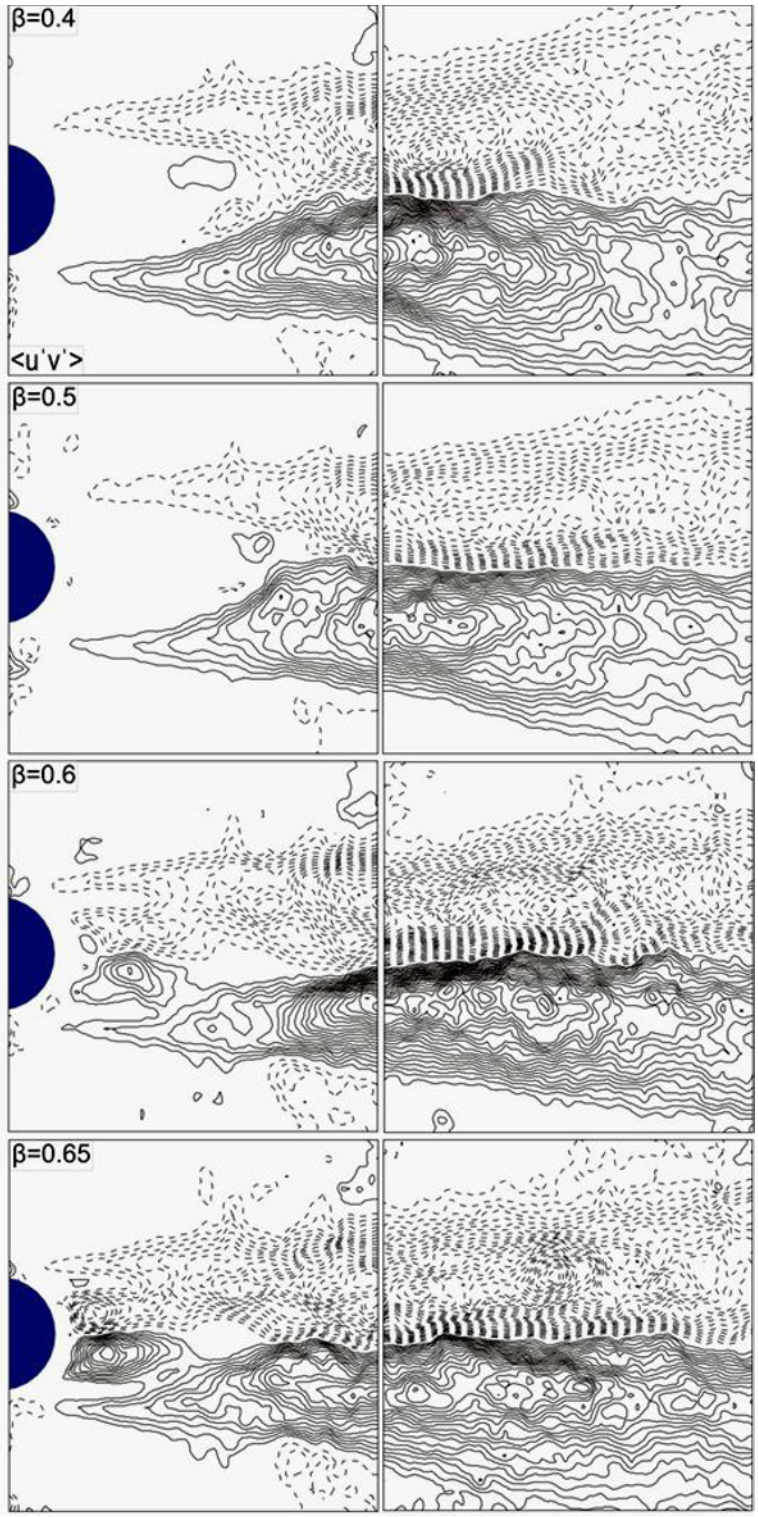
β=0.4
<u'v'>
β=0.5
β=0.6
β=0.65

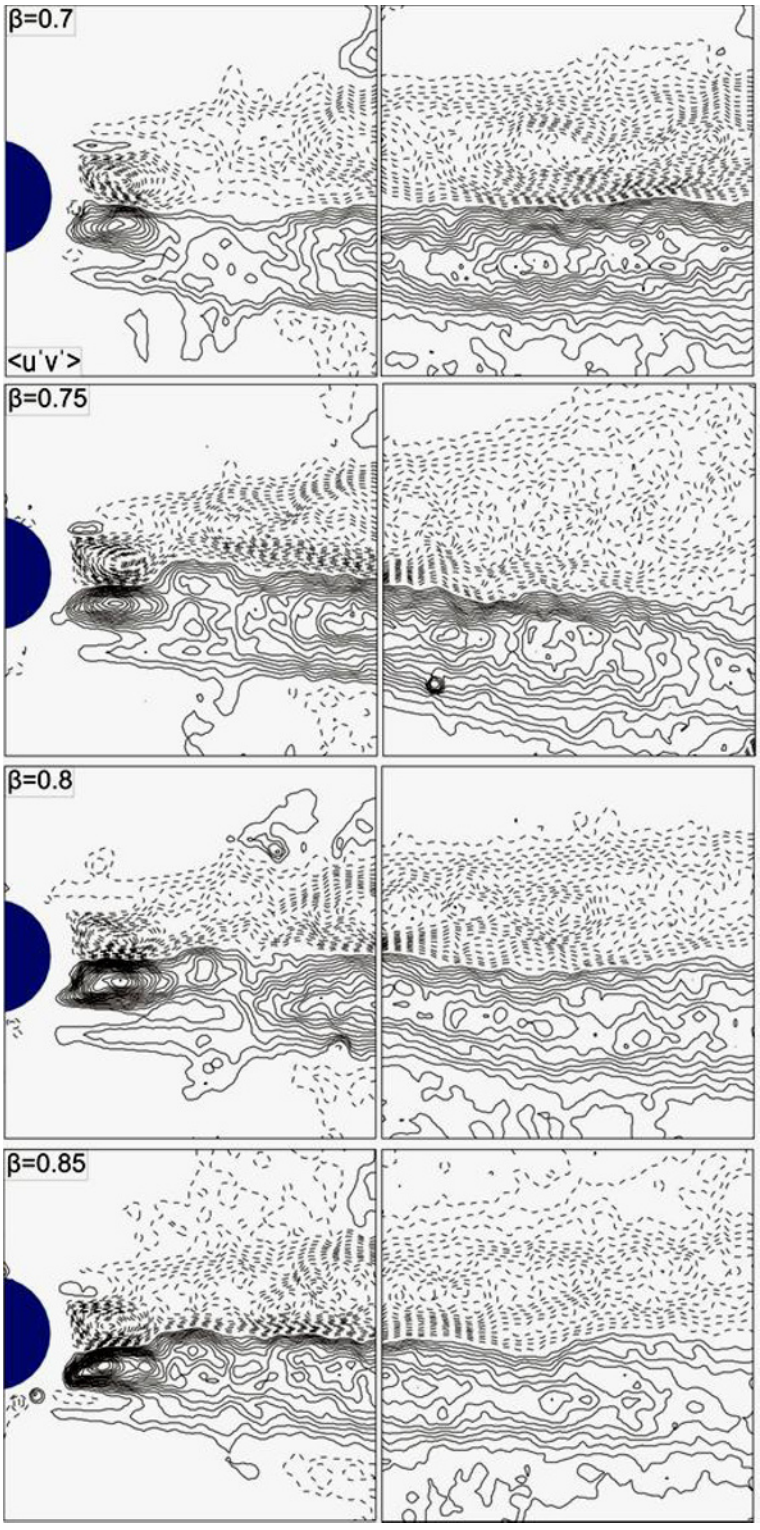


**Fig. 5.** The Reynolds stress contours for different porosities

Figure 5 presents contours of normalized Reynolds Stress $\langle u' v' / U^2 \rangle$ for all porosities, $0.4 \leq \beta \leq 0.85$. The minimum and incremental values of Reynolds Stress are taken as ± 0.001 and 0.001, respectively. Figure 5 indicates that the outer porous cylinders have significant effect on the control of flow downstream of the inner cylinder-outer cylinder arrangement. For the porosity range of $0.4 \leq \beta \leq 0.65$, the location of maximum Reynolds stress moves away from the cylinders arrangement and the maximum Reynolds stress occurs in the second view field. For $\beta = 0.40$ and 0.50, the outer porous is completely effective on the inner cylinder. The occurrence of Von-Kármán vortex street is prevented. The wake region behind the cylinders extends along the streamwise direction. For these porosities, the reduction of the magnitude of maximum Reynolds stress compared to the bare cylinder case is about 50%. For higher porosities $\beta > 0.5$, the outer porous cylinder loses the efficiency on the inner cylinder. But the positive effect of the outer cylinder on the flow control keeps on. The Reynolds stress contours

generated by the inner cylinder covers the wake region. The concentration of Reynolds stress decreases significantly compared to the bare cylinder case and the magnitude of maximum Reynolds stress reduces to 60% of that of the bare cylinder in the first view field except the porosities $\beta$ = 0.80 and 0.85. Due to the fact that the Reynolds stress contours generated by the inner cylinder have increased peak values of the Reynolds stress than those of the generated by the outer cylinder for the higher porosities $\beta$ > 0.65, the maximum Reynolds stresses are formed in the first view area.

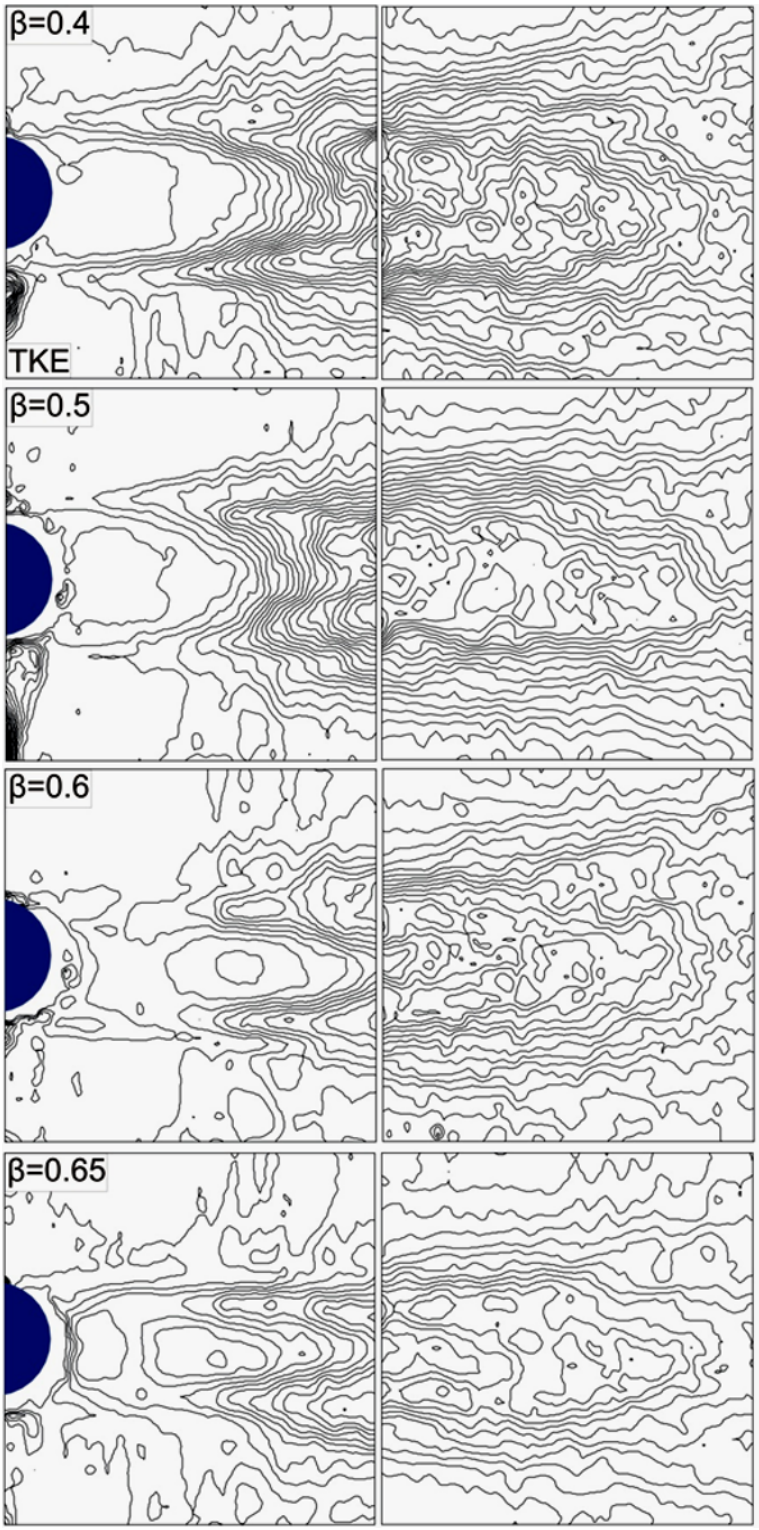

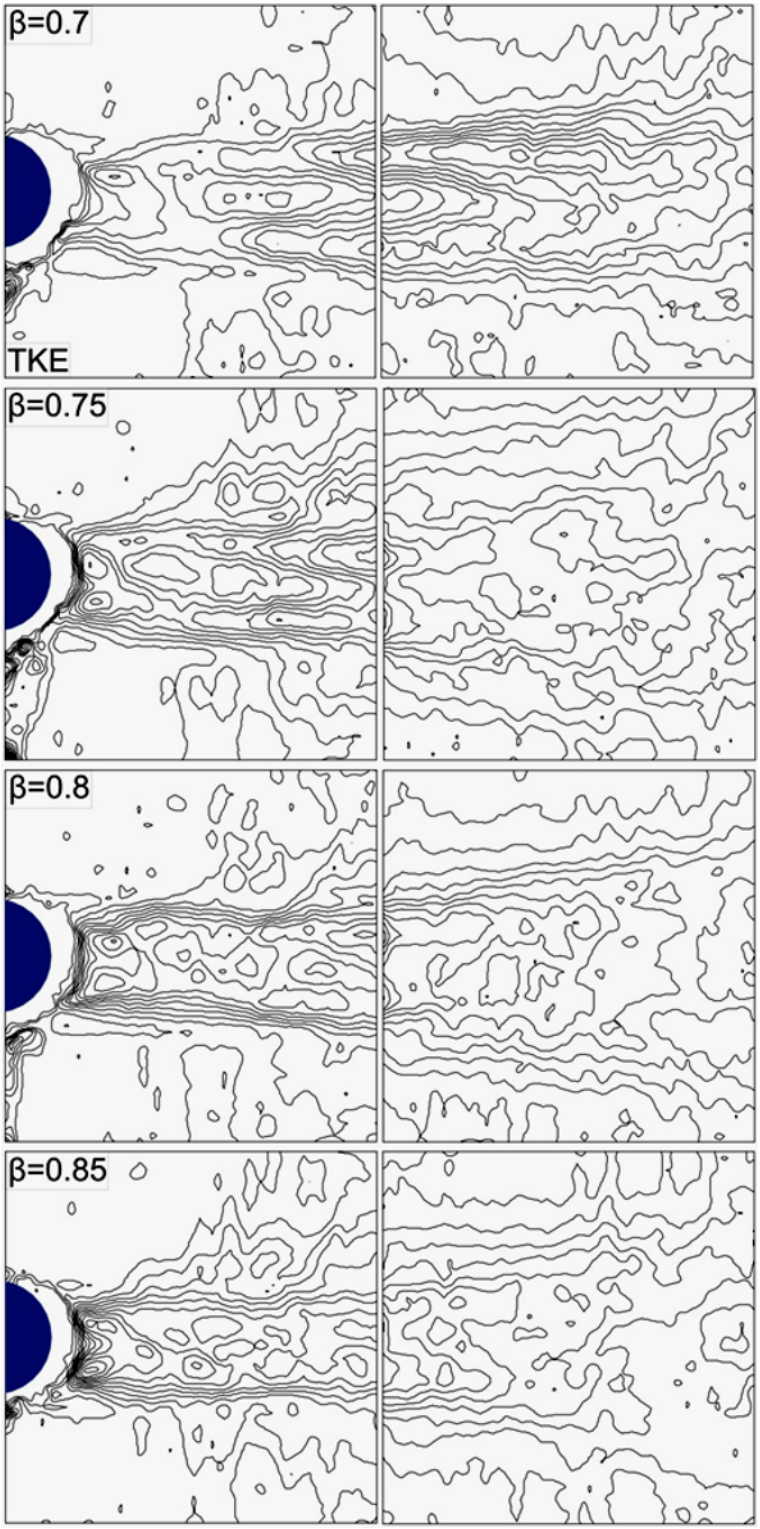


**Fig. 6.** The turbulent kinetic energy contours for different porosities

Turbulent kinetic energy contours are indicated in figure 6 to understand the flow information about the turbulence intensity of the flow field. For all porosities, it is obviously seen that the concentration of the turbulent kinetic energy decreases compared to the bare cylinder in the first flow field, whereas it increases in the second view field. The peak value of TKE is reduced to approximately 50-60% of that of the bare cylinder as the maximum value of Reynolds stress contours. The outer porous cylinder diminishes the concentration of the turbulent kinetic energy in the middle of the wake region for the porosities $\beta$ = 0.40 and 0.50. However, high concentrations of turbulent kinetic energy can be seen along the shear layer. The increase in the turbulent kinetic energy along the shear layers means that the effectiveness of the Kelvin-Helmholtz vortices is greater due to the higher velocity difference between the wake region and the free stream flow. For higher porosities $\beta \geq 0.60$, the concentration of the TKE increases in the field adjacent to the inner cylinder-outer cylinder arrangement.

## 4 Conclusions

The purpose of this study is to control the flow downstream of a circular cylinder in deep water using a surrounding outer porous cylinder. The results obtained in this study demonstrate that the unsteady flow downstream of the cylinder is controlled and turbulent intensity is reduced considerably for all porosities in the first view field. For higher porosities $\beta > 0.5$, the outer porous cylinder loses the efficiency on the inner cylinder. But the positive effect of the outer cylinder on the flow control keeps on. The porosities $\beta = 0.4$ and 0.5 are most suitable cases to control the flow downstream of the circular cylinder. For these porosities, the occurrence of Von-Kármán vortex street is prevented. The wake region behind the cylinders extends along the streamwise direction.

## References


1. S.J. Lee, H.B. Kim, J. Wind Eng. Ind. Aerod. **71**, 351-361 (1997)
2. A. Kahraman, B. Sahin, D. Rockwell, Exp. Fluids, **33**, 54-65 (2002)
3. H-C. Lim, S-J. Lee, Fluid Dyn. Res. **35**, 107-122 (2004)
4. S.J. Lee, S.I. Lee, C.W. Park, Fluid Dyn. Res. **34**, 233–250 (2004)
5. H. Akilli, B. Sahin, N.F. Tumen, Flow Meas. Instrum. **16**, 211–219 (2005)
6. H. Akilli, C. Karakus, A. Akar, B. Sahin, N.F. Tumen, J. Fluid Eng-T ASME, **130**, 1-11 (2008)
7. S. Bhattacharyya, S. Dhinakaran, A. KHALILI, Chem. Eng. Sci. **61**, 4451-4461 (2006)
8. A. Anderson, A.A. Szewczyk, Exp. Fluids, **23**, 161-174 (1997)
9. S.B. Yucel, O. Cetiner, M.F. Unal, Exp. Fluids, **49**, 241-255 (2010)
10. B. Stappenbelt, Int. J. Offshore Polar, **20**, 190-195 (2010)
11. C.H. Bruneau, I. Mortazavi, Int. J. Numer. Meth. Fluids, **46**, 415–433 (2004)
12. C. Hu, Y. Zhou, Aerodynamic Characteristics of Asymmetric Bluff bodies, J. Fluid Eng. **131**, 011206-9 (2009)
13. S. Bhattacharyya, A. K. Singh, Int. J. Numer. Meth. Fluids, **65**, 683–698 (2011)
14. O-S Gim, S-H. Kim, G-W. Lee, Ocean Eng. **38,** 2171–2184 (2011)
15. R. Galvaoa, E. Leea, D. Farrella, F. Hovera, M. Triantafylloua, N. Kitneyb, P.Beyne, J. Fluid Struct. **24,** 1216–1226 (2008)
16. M. Schumm , E. Berger, P.A. Monkewitz, J. Fluid Mech. **271,** 17-53 (1994)
17. B. Sahin, N.A. Ozturk, Measurement, **42,** 225–240 (2009)